Proceedings of IMECE2005
2005 ASME International Mechanical Engineering Congress and Exposition
November 5-11, 2005, Orlando, Florida USA

IMECE2005-80223

ELECTROKINETIC FOCUSING AND DISPENSING OF PARTICLES AND CELLS ON MICROFLUIDIC CHIPS

Xiangchun Xuan, Edmond W.K. Young and Dongqing Li
Department of Mechanical and Industrial Engineering, University of Toronto, 5 King's College Road, Toronto, Ontario, Canada, M5S 3G8
Email: dli@mie.utoronto.ca

ABSTRACT

This work investigated the electrokinetic focusing and dispensing of polystyrene particles and red blood cells on microfluidic chips. Particles or cells were first electrokinetically focused using the merging of focusing streams on the sample stream, and subsequently separated as a result of the focusing. These particles or cells were then selectively dispensed from the focused sample stream using precise application of electrical pulses. The whole process of focusing, separation and dispensing of particles was visualized by a custom-made microscopy system. In particular, the width of the focused fluorescein stream and the accelerated electrophoretic motion of particles and cells were measured in a cross-channel and compared with a proposed analytical model. The electrokinetic manipulation of particles and cells demonstrated in this work can be used for developing integrated lab-on-a-chip devices for studies of cells.

INTRODUCTION

Lab-on-chip devices have been widely used to manipulate liquid flows on chips for counting and sorting particles or cells [1-3]. These particles or cells are first focused to flow in a single file passing the detection region. The targeted ones are then deflected from the sample stream for the subsequent analysis.

Generally the particle/cell focusing can be realized by two approaches: passive focusing uses converging channels to line particles or cells without additional energy source [4,5], and active focusing uses externally driven side streams to confine the sample stream. In the latter approach, both pressure drop (named as hydrodynamic focusing in the literature) [6-8] and electrical field [9-11] (named as electrokinetic focusing) have been used to drive the focusing streams. The accelerated motion of particles or cells through the focusing region that is crucial to the subsequent counting and sorting, however, has received little attention. These motions may be significantly different from those at the macro-scale due to the strong interfacial and boundary effects involved in such microchannel-liquid-particle/cell systems, especially for the case of electrokinetic focusing [12]. These effects have been demonstrated in our recent experiments [13-15].

The subsequent microfluidic particle/cell sorting is commonly achieved by the active control of either the fluid flow or the particle/cell motion itself. The switch of fluid flow has been implemented by either electrokinetic [5,11,16] or hydrodynamic means [8,17,18] or their combination [19]. Dielectrophoretic [20] and optical forces [21] have also been applied directly onto targeted particles or cells to realize the active sorting.

In this work, we first investigate the electrokinetic focusing and the accelerated electrophoretic motion of focused particles and cells in microfluidic cross-channels. We then demonstrate, in a simple double-cross microchannel, the selected electrokinetic dispensing of single particles or cells from the electrokinetically focused sample stream.

MATERIALS AND METHODS

Fluorescent polystyrene microspheres of 5.7 μm (referred to as 6 μm particles hereafter), and 10.35 μm (referred to as 10 μm particles hereafter) in diameter were purchased from Bangs Laboratory (Fisher, IN) in the form of 1% solid suspension in pure water. Both particle solutions were further diluted with pure water by 50 times, and gently vibrated prior to use because particles are slightly heavier than water (nominal density is 1.05 g/ml). The powder of rabbit red blood cells (approximately 6 μm in diameter) was dissolved in pure water. As per the product manual from Sigma-Aldrich (Louis, MO), these are "fixed" cells that do not swell up in pure water. The cell solution was diluted to approximately the same concentration as 6 μm particles with pure water. To demonstrate the electrokinetic focusing, fluorescein (332.31 MW, Molecular Probes, Eugene, OR) was dissolved to 50 μM in 10 mM sodium buffer solution of pH = 8.5. This solution was filtered

using 0.22 μm pore size syringe filters immediately before use. Microfluidic cross-channels were fabricated in PDMS using the soft lithography technique [22]. The detailed procedure is described elsewhere [15].

The electrokinetic focusing and the electrophoretic motion of particles and cells were adjusted by a high-voltage DC power source (Glassman High Voltage, Inc., High Bridge, NJ) in conjunction with a custom-made voltage controller. Pressure-driven flows were eliminated by carefully balancing the liquid height in the reservoirs immediately before experiments. The fluorescein was continuously excited by a single-line argon laser (488 nm, 200 mW, American Laser Corp., Salt Lake City, UT), and the emitted fluorescent signal was collected by a 32×, NA (numerical aperture) = 0.60 microscope objective. In visualizing the focused electrophoretic motion of particles and cells, however, a direct-current lamp lit the view window from the back. The resultant transmitted signal was collected by a 16×, NA = 0.30 microscope objective for larger fields of view. All optical signals were captured by a progressive scan CCD camera (Pulnix America Inc., Sunnyvale, CA) running in video mode at 15 Hz. The acquired images were normalized by a bright field image after subtracting the background noise. The intensity of these images was then scaled to fill the grayscale range. The information of particle or cell centers with respect to time was manually extracted from the processed images.

THEORY

In this section simple formulae are developed for predicting the width of the focused stream and the accelerated electrophoretic motion of focused particles and cells in cross-microchannels. Fig. 1 shows the channel structure and the diagram of the corresponding resistive circuit. According to Kirchoff's 1st law, we should have [23]

$$I_i + 2I_f = I_o \tag{1}$$

$$Q_i + 2Q_f = Q_o \tag{2}$$

where I and Q signify the electrical current and the flow rate, and the subscript f, i and o indicate the focusing channel, inlet channel and outlet channel, respectively.

The electrical current in an electrokinetic flow is composed of two parts: one is the streaming current due to the motion of charged ions carried by the bulk fluid, and the other is the conduction current due to the ion electrophoretic motion [12]. The former is generally much smaller than the latter unless the channel size is comparable to the thickness of electrical double layers (on the order of nanometers), indicating that

$$\frac{V_i - V}{\gamma R} + 2\frac{\alpha V_i - V}{R} = \frac{V}{\beta R} \tag{3}$$

where V_i is the voltage imposed to the reservoir of the inlet channel, V is the voltage in the cross intersection, R is the electrical resistance of the focusing channel, γ and β are the ratios of electrical resistances of the inlet and outlet channels to that of the focusing channel, and α is the ratio of applied voltage at the focusing channel to that at the inlet channel. Eq. (3) gives rise to

$$V = \frac{\beta + 2\beta\gamma\alpha}{\beta + \gamma + 2\beta\gamma} V_i . \tag{4}$$

It is apparent from Fig. 1 that $V \le V_i$ and $V \le \alpha V_i$ should be obeyed simultaneously in order to realize the electrokinetic focusing in the cross-channel, which in turn determines the lower and higher limits of the voltage ratio α,

$$\alpha_{\min} = \frac{\beta}{\beta + \gamma} \tag{5}$$

$$\alpha_{\max} = 1 + \frac{1}{2\beta} . \tag{6}$$

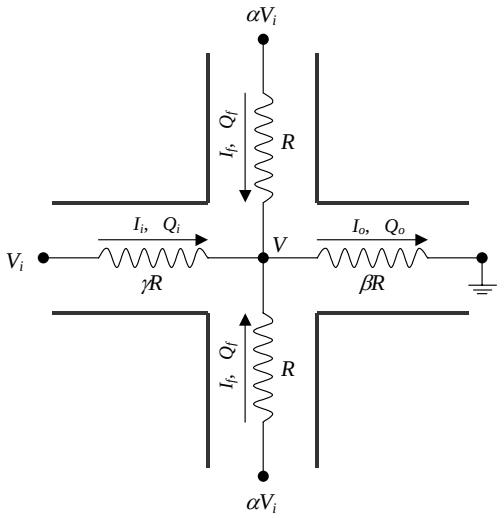

Fig. 1: The diagram of the resistive circuit corresponding to electrical current and fluid flow in the microfluidic cross-channel.

It is easy to understand that γ and β essentially reflect the length ratios of the inlet and outlet channels to the focusing channel if all channels have exactly the same cross-section. Hence, Eq. (1) or (3) is equivalent to

$$E_i + 2E_f = E_o \tag{7}$$

where E denotes the electrical field strength. The electrokinetic flow rate in each channel may also have two components: one is due to the electroosmotic flow in response to the electrical field given in Eq. (7), and the other is from the induced pressure-driven flow, if any, in order to satisfy the mass continuity [12]. In the limit of thin electrical double layers the electroosmotic velocity is proportional to the electrical field by a coefficient, i.e., the so-called electroosmotic mobility that is uniform in the current cross-microchannel. As such, Eq. (7) ensures that the flow rate due to the electroosmotic flow has already satisfied the mass conservation in Eq. (2). In other words, there is no induced pressure-driven flow in this cross-channel, indicating a full-field similarity between the electrical and velocity fields [24].

In electrokinetic focusing, the inlet stream is squeezed by the focusing streams in the cross intersection and subsequently forms a focused stream in the outlet channel. Assuming a rectangular cross-section of the focused stream, it is straightforward to obtain the following focusing ratio

$$\frac{w_f}{w} = \frac{E_i}{E_o} \tag{8}$$

where w and w_f denote the width of the inlet channel and the focused stream, respectively. Incorporating Eq. (4), the ratio of electrical field in Eq. (8) is specified as,

$$\frac{E_i}{E_o} = \frac{(V_i - V)/\gamma}{V/\beta} = \frac{1 + 2\beta - 2\beta\alpha}{1 + 2\gamma\alpha}. \qquad (9)$$

Therefore, a tighter focusing can be achieved by increasing γ, the ratio of the inlet channel resistance (or equivalently, the length) to the focusing channel resistance. For the focused particles and cells, their electrophoretic motions are proportional to the electrical field by a coefficient that is dependent on the system (including channel, liquid and particles or cells) properties and the channel geometry as well as the particle location [12,25]. In the inlet and outlet channels far away from the cross intersection, however, this coefficient is identical. Therefore, the accelerated electrophoretic velocity of particles and cells, U_f, after focusing is described by

$$\frac{U_f}{U_p} = \frac{E_o}{E_i} \qquad (10)$$

where U_p is the particle or cell velocity in the inlet channel.

RESULTS AND DISCUSSION

Cross-microchannels were used to study the electrokinetic focusing and the focused electrophoretic motion of particles and cells. Double-cross microchannels were used to demonstrate the electrokinetic dispensing of single particles or cells. The channel structures are specified below.

Electrokinetic focusing

In the focusing experiments, the four branches of the cross-microchannel are all 20 μm deep and 120 μm wide and 12.5 mm long. Thus, the ratios β and γ defined in the preceding section (see Fig. 1) are both equal to 1. The lower and higher limits of the voltage ratio α given in Eqs. (5) and (6) are hence 0.5 and 1.5, respectively. In the experiments, the voltage V_i applied to the inlet channel was always fixed to 300 V while the voltage at the focusing channel was varied between 150 V and 450 V (accordingly, $0.5 \le \alpha \le 1.5$).

Fig. 2a demonstrates the electrokinetic focusing where the fluorescein was moving from left to right. For the images from top to bottom, the voltage ratios α are 2/3, 2.5/3, 1, 3.5/3 and 4/3 in order. Apparently, as α is increased, the width of the focused stream narrows. This is attributed to the larger squeeze of the inlet streamlines or equivalently the inlet electrical field lines in the cross intersection. Fig. 2b shows the calculated electrical field lines through the intersection at α = 2/3, 1 and 4/3 in order from top to bottom. This simulation was performed in FLUENT at the experimental conditions. The close agreement between the experimentally observed fluorescent images and the simulated electrical field lines justifies the similarity between the electrical and velocity fields. The complicated calculation of concentration field in such microchannel networks is therefore unnecessary. We also measured the widths of the focused fluorescein stream (full rectangles) at different α, which agree well with the theoretical prediction (solid line with a left arrow) from Eq. (8) within the experimental error, as shown in Fig. 3. The smallest measured focusing width is approximately 7 μm (or $w_f/w \approx 0.06$) at α = 1.4 (not shown in Fig. 2a). Higher α values were not used because the focused fluorescein was too weak to be distinguished from the background in the current setup.

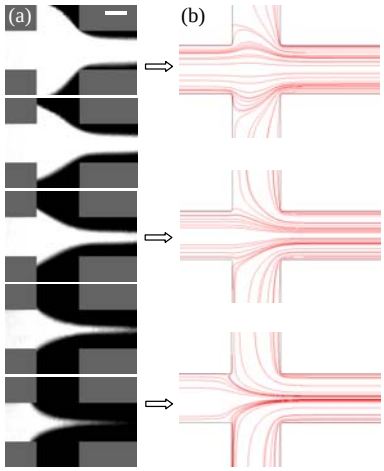

Fig. 2: Electrokinetic focusing in a microfluidic cross-channel: (a) fluorescent images at the voltage ratio α = 2/3, 2.5/3, 1, 3.5/3, and 4/3 from top to bottom; (b) numerically calculated electrical field lines at α = 2/3, 1, and 4/3 in order from top to bottom. The scale bar on the top image represents 50 μm.

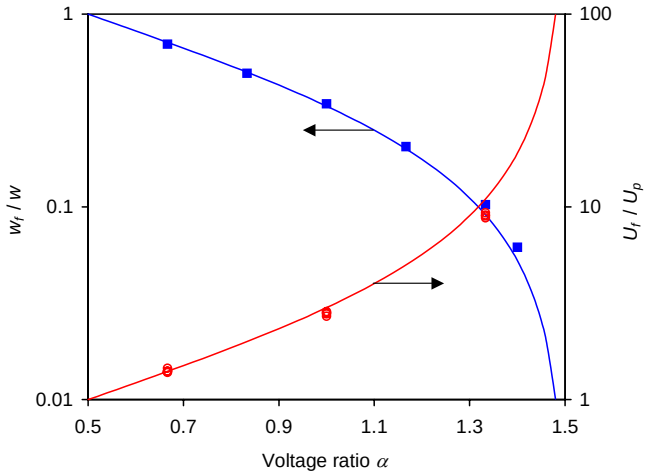

Fig. 3: Comparison of the experimentally measured focusing ratio w_f / w (full rectangles, corresponding to the left ordinate) and particle acceleration U_f / U_p (hollow circles, corresponding to the right ordinate) with theoretical predictions (solid lines) at different voltage ratio α. Note that for U_f / U_p at each α, four different particles were extracted corresponding to four data points (i.e., four circles).

Focused electrophoretic motion of particles and cells

Fig. 4 shows the images of electrokinetically focused 6 μm particles at different ratios of α. Consistent with the fluorescent images in Fig. 2a, particles were more tightly focused as α is increased. Especially at α = 4/3, particles were well separated after the focusing because they were dramatically accelerated. This separation should be beneficial to the subsequent counting and sorting of particles. Next, we will examine the effects of voltage ratio α, particle size and particle property (i.e., polystyrene particle or red blood cell), and particle trajectory (specifically, particle position before focusing) on the accelerated electrophoretic motion of the focused particles and cells. To realize this objective, the particle and cell solutions

were extremely diluted so that particle-particle interactions (or cell-cell interactions) are negligible in the following analysis.

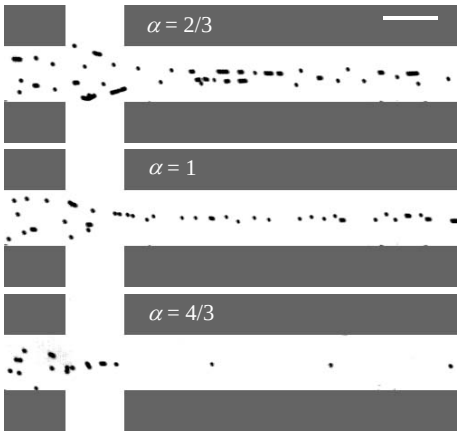

Fig. 4: Demonstration of electrokinetic focusing with concentrated 5 μm particles at different voltage ratios α. The scale bar on the top image represents 100 μm.

Effect of voltage ratio α

Fig. 5a shows the trajectories of 10 μm particles moving along the channel centerline at different α. The particle trajectory is obtained by superimposing sequential images of a single particle. The time interval between adjacent images (i.e., the time interval between adjacent particles in the trajectory) is 1/15 s. Note that the small curvature of particle trajectory in the channel intersection for the cases of α = 2/3 and 4/3 is attributed to the slight departure of particles from the channel centerline in the inlet channel. As α is increased, particles slow down before the cross intersection, i.e., before the electrokinetic focusing, and speed up after the intersection. The particle velocity variations (symbols, referring to the left ordinate) across the intersection are shown in Fig. 5b where the two vertical lines indicate the two edges of the focusing channel. When α varies from 2/3 to 4/3, the particle velocity before the electrokinetic focusing is reduced three-fold while enhanced by 50% after the focusing. Therefore, particles achieve a larger acceleration when α increases. The particle velocity ratios (hollow symbols) before and after the focusing are summarized in Fig. 3, and agree well with the theoretical predictions (solid line with a right arrow) from Eq. (10) within experimental error. At α = 4/3 (see the bottom image in Fig. 4), for example, the experimentally measured particle velocity could be accelerated by approximately 8 times after the electrokinetic focusing.

Another interesting feature in Fig. 5b is particle velocity attains a minimum close to the intersectional center at α = 2/3. For the other two α values, however, no such extreme point appears in the velocity curves. We also note that the position from which the particle acceleration starts is pushed upstream as α is increased. These phenomena can be well explained with the distribution of axial electrical field (solid lines, referring to the right ordinate) along the channel centerline as shown in Fig. 5b. However, the starting and ending positions of particle acceleration are slightly shifted to the downstream with respect to the axial electrical field, especially at higher α. This shift might be attributed to the dielectrophoretic force that is generated by the non-uniform electrical field in the channel intersection [26]. This force points to the lower electrical field region and thus tends to retard the particle electrophoretic motion. At a higher α, the electrical field gradient grows larger in the intersection resulting in a stronger dielectrophoretic force. This force is also dependent on the particle size and permittivity, whose effect will be discussed in the next section.

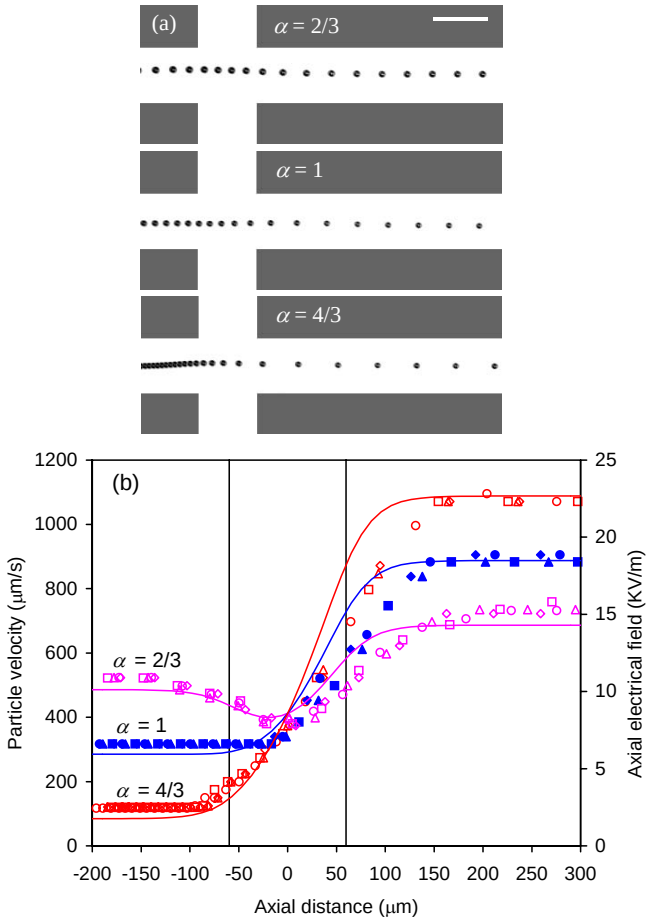

Fig. 5: The effect of voltage ratio α on the focused electrophoretic motion of 10 μm particles along the centerline of a microfluidic cross-channel: (a) particle trajectories with 1/15 s intervals between adjacent particles; (b) particle velocity variations (symbols, referring to the left ordinate) across the channel intersection where four individual particles are selected for each value of α. The three curves (solid lines, referring to the right ordinate) display the distributions of numerically calculated axial electrical field along the horizontal centerline of the cross-channel at the experimental conditions. The two vertical lines in (b) indicate the two edges of the focusing channel. The scale bar on the top image represents 100 μm.

Effect of particle size and property

Fig. 6a shows the trajectories of a 10 μm particle, 6 μm particle and red blood cell migrating along the channel centerline at the voltage ratio α = 1. The time intervals between adjacent particles in the trajectories are 1/15 s. Both particles and cells underwent an acceleration in the cross intersection. Their velocity variations across the intersection are illustrated

in Fig. 6b. While the absolute magnitude of velocity is different due to the discrepancy in surface potential, all particles and cells attain approximately the same degree of acceleration, i.e., U_f / U_p ≈ 2.7, after the electrokinetic focusing. Namely, this acceleration is insensitive to the particle size and property (i.e., particle or cell) under the experimental conditions. However, the acceleration region of 10 μm particles seems to be further shifted to the downstream, although not obvious, compared to that of 6 μm particles and red blood cells (approximately 6 μm in diameter). This deviation might again be attributed to the aforementioned dielectrophoretic force that is proportional to the particle volume.

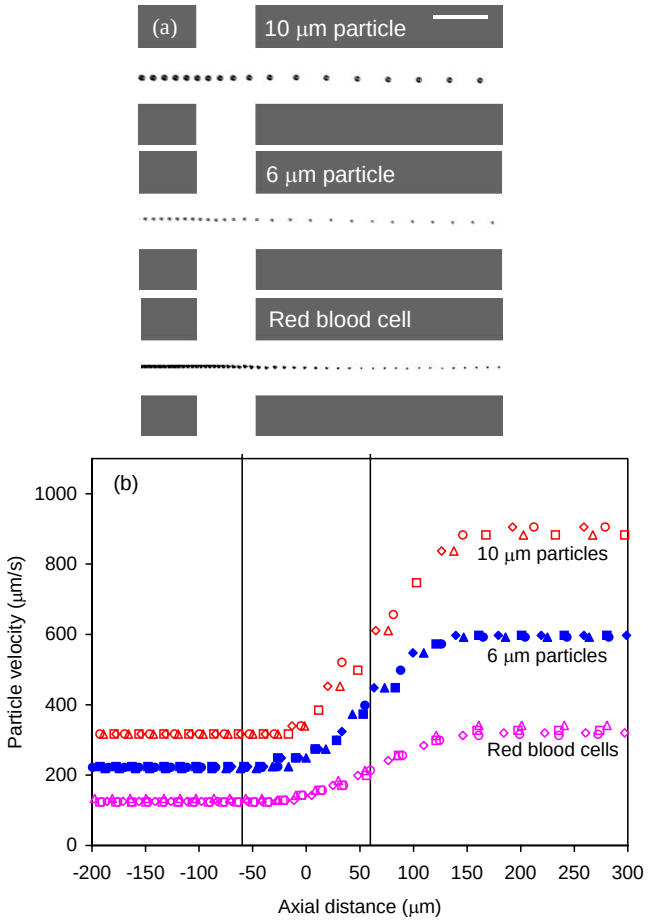

Fig. 6: The effect of particle size and property on the focused electrophoretic motion of particles and cells along the centerline of a microfluidic cross-channel at the voltage ratio α = 1: (a) particle trajectories with 1/15 s intervals between adjacent particles; (b) particle velocity variations across the channel intersection where four individual particles or cells are selected for each case. The two vertical lines in (b) indicate the two edges of the focusing channel. The scale bar on the top image represents 100 μm.

Effect of particle position before focusing

Fig. 7a shows the trajectories of electrokinetically focused 6 μm particles when they were moving at three different positions in the inlet channel, i.e., close to sidewalls (top), along the centerline (bottom), and intermediate region (middle). The voltage ratio was fixed at α = 1. After the electrokinetic focusing in the cross intersection, all three particles were observed approaching the centerline of the outlet channel as have been demonstrated in Fig. 4. Their velocity variations are summarized in Fig. 7b. One can see that all data points collapse to one curve that is similar to the distribution of axial electrical field (α = 1 curve in Fig. 5b) except those in the vicinity of the edge of the focusing channel, i.e., the left vertical line in Fig. 7b. This deviation is due to the locally lower electrical field around the corner as shown in the inset in Fig. 7b. Therefore, the particle position in the inlet channel has minor effect on the acceleration of focused electrophoretic motion.

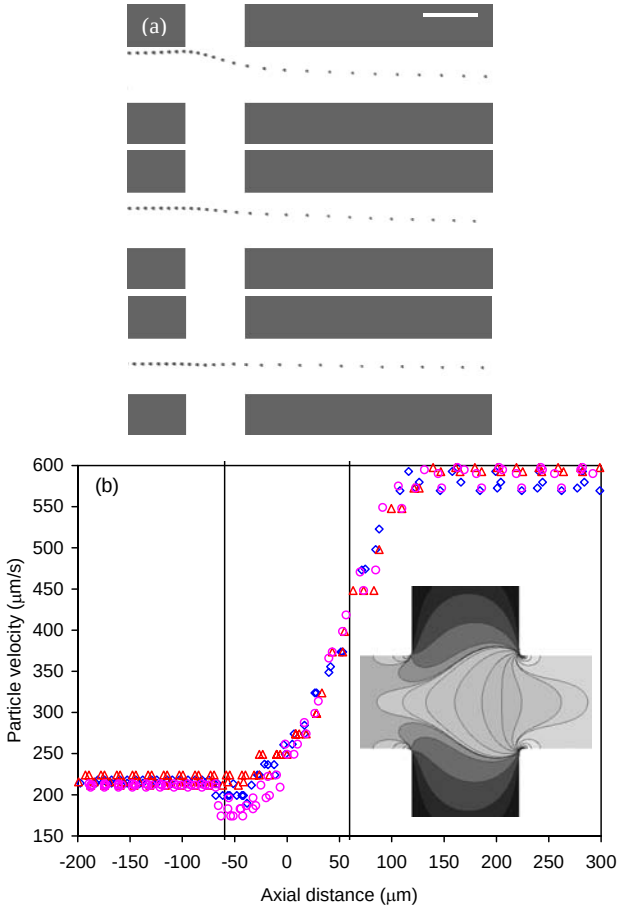

Fig. 7: The trajectory effect on the focused electrophoretic motion of 5 μm particles in a microfluidic cross-channel at α = 1: (a) particle trajectories with 1/15 s intervals between adjacent particles; (b) particle velocity variations across the channel intersection where four individual particles are selected for each trajectory (triangles for particles close to centerline, circles for those close to sidewalls, and diamonds for those in between centerline and either sidewall). The two vertical lines in (b) indicate the two edges of the focusing channel. The inset is a contour of axial electrical field in the intersection (darker region indicating smaller field strength).

Electrokinetic dispensing of single particles/cells

Fig. 8 is a photograph of the double-cross microchannel for the electrokinetic dispensing of single particles or cells. A dispensing channel of 50 μm in width and of the same depth as other channels is 0.8 mm downstream from the focusing intersection, through which an electrical pulse could be

instantly triggered to dispense a targeted particle or cell. A delay generator (Stanford Research Systems, Sunnyvale, CA) controlled the firing time and the duration of the electrical pulse. In the normal operating mode, 300 V was applied at the reservoirs of the inlet and focusing channels, the reservoir of the outlet channel was grounded, and the reservoir of the dispensing channel was left floating. On switching to the dispensing mode, a 300 V potential drop was applied to the dispensing channel while all other channels were floating. We mixed the 6 μm and 10 μm particle solutions used in the earlier focusing experiments and then tried to move only the 10 μm particles to the dispensing channel. A sequence of four images in Fig. 9 shows the typical dispensing process of a single 10 μm particle with a 0.3 s electrical pulse. The time interval between adjacent images (from top to bottom) is 0.2 s. In this proof-of-concept experiment, the targeted 10 μm particles were identified by the naked eye.

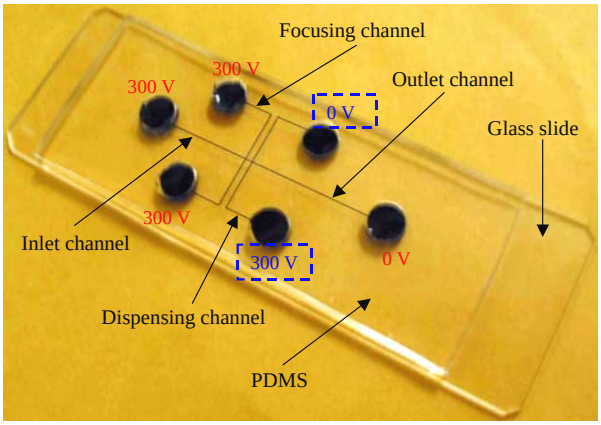

Fig. 8: Photograph of the microfluidic chip for electrokinetic focusing and dispensing of particles and cells. The channel was filled with dark blue food dye for a clear demonstration. The voltage values indicate the electrical potentials applied to the adjacent reservoirs, of which those without dashed box are for the normal operating mode while those with dashed box are for the dispensing mode. In each mode, the reservoirs without designated potentials are floating.

It is noted that within the short period of electrokinetic dispensing, fluid and particles outside the dispensing channel remained stationary and thus remained focused (see Fig. 9). This feature ensures that no desired particles or cells will be missed during the dispensing process. However, the stagnation of fluid and particles certainly reduces the sorting throughput. The minimum time period of stagnation, i.e., the duration of electrical pulse, is mainly restricted by three factors: the amplitude of electrical pulse, the difference in surface potentials of the channel and the targeted particle, and the velocity of the focused stream in the outlet channel in the normal operating mode. The first two factors determine the velocity of the dispensed particles while the last one governs the "pulling back" force exerted on the dispensed particles once the flow switches back to that in the normal operating mode. Therefore, if fluid and particles move faster in the outlet channel, a longer electrical pulse should be applied to ensure that the dispensed particles could fully escape from the focused stream. We estimate that the throughput in the current experiment is up to 10 particles/cells per second if the number ratio of the dispensed particles to total particles is 0.2. This sorting speed can be increased by increasing the applied voltages, and by adding multiple microchannel structures in the same chip. The practical electrical fields are, however, restricted by Joule heating effects that may denature or even lyse biological tissues [27], especially when physiological salt solutions (*e.g.*, 0.9% NaCl solution) with a high electrical conductivity are required to balance the osmotic pressures across the membrane of live cells. The purity of the sorted particles or cells is another concern. Apparently, higher sorting purity can be achieved with the highly-focused and well-separated particles, like those at $\alpha = 4/3$ shown in Fig. 5a.

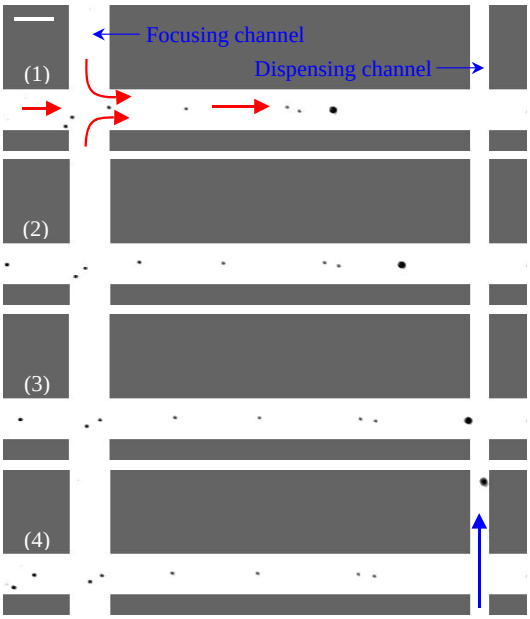

Fig. 9: Image sequence of the electrokinetic dispensing of a single 10 μm particle. The time interval between adjacent images (from top to bottom) is 0.2 s. The duration of the electrical pulse for dispensing is 0.3 s. The arrows inside channels indicate the flow directions. The scale bar on the top image represents 100 μm.

CONCLUSIONS

We have investigated the electrokinetic focusing and the focused electrophoretic motion of particles and cells in cross-microchannels. The width of the focused fluorescein stream and the velocity of the focused particles and cells were measured. The ratios of stream width and particle/cell velocity in the outlet channel to those in the inlet channel both agree well with the proposed analytical formulae. The increase of particle velocity after focusing is determined by the voltage ratio α and insensitive to the particle size, particle property (i.e., polystyrene particles or red blood cells) and particle trajectory. Also, the particle velocity variation through the channel intersection was tracked and follows a similar trend to the distribution of axial electrical field. However, the region of particle acceleration seems to be pushed downstream in the velocity curve, especially for large particles at high voltage ratios. This shift might be attributed to the dielectrophoretic force that is generated by the non-uniform electric field in the

channel intersection. We have also proposed an electrokinetic means to selectively dispense single particles or cells from the focused sample stream. This totally electrokinetic manipulation of particles demonstrated in a double-cross microchannel will facilitate developing integrated lab-on-a-chip devices for studies of single cells.

ACKNOWLEDGMENTS

Financial support from the Natural Sciences and Engineering Research Council (NSERC) of Canada, through a research grant to D. Li is gratefully acknowledged.

REFERENCES

[1] Reyes, D. R.; Iossifidis, D.; Aurous, P.; Manz, A. *Anal. Chem.* **74**, 2623-36 (2002).
[2] Stone, H. A.; Stroock, A. D.; Ajdari, A. *Annu. Rev. Fluid. Mech.* **36**, 381-411 (2004).
[3] Verpoorte, E. *Lab Chip* **3**, 60N-68N (2003).
[4] Jacobson, S. C.; Culberston, C. T.; Daler, J. E.; Ramsey, J. M. *Anal. Chem.* **70**, 3476-80 (1998).
[5] Fu, Y.; Spence, C.; Scherer, A.; Arnold, F. H.; Quake, S. R. *Nature Biotech.* **17**, 1109-11 (1999).
[6] Lee, G.; Lin, C.; Chang, G. *Sens. Actuat. A* 2003, *103*, 165-70.
[7] Pabit, S. A.; Hagen, S. J. *Biophys. J.* **83**, 2872-8 (2002).
[8] Wolff, A.; Perch-Nielsen, I. R.; Larsen, U. D.; Friis, P. et al. *Lab Chip* **3**, 22-7 (2003).
[9] Jacobson, S. C.; Ramsey, J. M. *Anal. Chem.* **69**, 3212-7 (1997).
[10] Fu, L.; Yang, R.; Lee, G. *Anal. Chem.* **75**, 1905-10 (2003).
[11] Dittrich, P. S.; Schwille, P. *Anal. Chem.* **75**, 5767-74 (2003).
[12] Li, D. *Electrokinetics in microfluidics*, Elsevier Academic Press, Burlington, MA, 2004.
[13] Xuan, X.; Li, D. 2004 (submitted)
[14] Xuan, X.; Ye, C.; Li, D. *J. Colloid. Interf. Sci.* **289**, 286-90 (2005).
[15] Xuan, X.; Xu, B.; Li, D. *Anal. Chem.* 2005 (in press).
[16] Li, P. C. H.; Harrison, D. J. *Anal. Chem.* **69**, 1564-8 (1997).
[17] Blankenstein, G.; Larsen. U. D. *Biosens. Bioelectron.* **13**, 427-38 (1998).
[18] Fu, A. Y.; Chou, H.; Spence, C.; Arnold, F. H.; Quake, S. R. *Anal. Chem.* **74**, 2451-7 (2002).
[19] Johann, R.; Renaud. *Electrophoresis* **25**, 3720-9 (2004).
[20] Fideler, S.; Shirley, S. G.; Schnelle, T.; Fuhr, G. *Anal. Chem.* **70**, 1909-15 (1998).
[21] Wang, M. M.; Tu, E.; Raymond, D. E.; Yang, J. M. et al. *Nature Biotech.* **23**, 83-7 (2005).
[22] Duffy, D. C.; McDonald, J. C.; Schueller, O. J. A.; Whitesides, G. M. *Anal. Chem.* **70**, 4974-84 (1998).
[23] Xuan, X.; Li, D. *J. Micromech. Microeng.* **14**, 290-298 (2004).
[24] Santiago, J. G. *Anal. Chem.* **73**, 2353-65 (2001).
[25] Ye, C.; Xuan, X.; Li, D. *Microfluid. Nanofluid.* **1**, 234-41 (2005).
[26] Pohl, H. A. *Dielectrophoresis*, Cambridge University Press, Cambridge, 1978.
[27] Rush, R. S.; Cohen, A. S.; Karger, B. L., *Anal. Chem.* **63**, 1346-50 (1991).